A Ready Reckoner of CFD for Wrap-around Fins

Nayhel SHARMA*,[1], Rakesh KUMAR[1]

*Corresponding author
[1]Aerospace Engineering Department, Punjab Engineering College
(Deemed to be University),
Sector 12, Chandigarh, 160012-India,
nayhel.sharma@gmail.com*, rakeshkumar@pec.ac.in

DOI: 10.13111/2066-8201.2019.11.2.13

Received: 28 November 2018/ Accepted: 21 March 2019/ Published: June 2019

Abstract: *This paper aims to review computational fluid dynamics (CFD) analysis of wraparound fins (WAF). An effort in the search of a benchmark computational fluid dynamics model for future studies has been made in this paper. Iterative studies have been carried out in the past to study the cause and effect of the anomalies in the aerodynamics of WAF missiles. The simulations that have been carried out consist of different geometries and different conditions, each providing us a new set of data, results and complexities. The results of the computations, their setups and the nuances of the simulations have been presented in this paper. This paper aids in validation of new CFD simulations with the previous CFD studies and their Experimental counterparts. Benchmarking of geometries, domain setup, grid generation, etc. will help to obtain a higher quality of the WAF aerodynamics visualization in the future.*

Key Words: *Computational Fluid Dynamics, Wrap-around Fins, Aerodynamics*

1. INTRODUCTION

The use of wraparound fins (WAF) in the aero-industry is becoming more relevant for the tube launched missiles. Having superiority over the conventional planar fins in terms of storage, these fins also show signs of reduced drag at higher angle of attacks and higher operational stability. The desire for obtaining an optimal design and identifying the root and cause of the discredits in WAF aerodynamics is a major concern of most researchers. These WAF show a conventional longitudinal aerodynamic characteristic like the planar fins having identical planform area. The major aerodynamic complication faced by the WAF is the production of rolling moment at zero angle of attack. The design of dynamically stable WAF demands the prediction of the roll moment coefficient for the whole flight path. The presence of inherent rolling motion is attributed to the missile geometry, fin geometry, Mach Number and the wake condition. It has been found that static aerodynamic characteristics of WAFs are very similar to a set of planar fins. The computational Fluid Dynamics (CFD) technology is a tested numerical simulation tool to solve such aerodynamic problems. The analyses have been performed on 2-D and 3-D geometries and from inviscid to viscous turbulent flows, etc. The advancements in the hardware and software have reduced the computational times and the computational costs. The various turbulent CFD models and their attributes have been discussed in this paper. These CFD numerical analyses are consistent with the experimental data of the wind tunnel tests as well as the free flight tests, however they lack accuracy. The dynamic instability is not caused by the unusual roll motion but instead have been reported

due to the presence of a side moment due to pitch, [2]. As the geometry is said to influence the aerodynamic characteristics of the curved fins, different length to diameter (l/d) ratios have been tested both experimentally and through CFD. The experimental missiles models generally were bimetallic bodies (brass nose and aluminium shaft) with steel fins which can be kept in mind while assigning material to the bodies in CFD. The center of gravity position has also been changed to simulate the real-time burnout condition of the missile [3]. Mathematical analysis through the missile programs predicts the characteristics of WAF based on similar projected area as that of planar fins. However, these programs are unable to analyse the side force and moment aerodynamics of the WAF. A study consisting of supersonics flow around a single WAF model mounted on a semi cylindrical model, has been carried out both numerically and experimentally which provided more insights into the WAF aerodynamics, [4], [5], [6], [7], [8]. This paper discusses the basic aerodynamics of the WAFs, its drawbacks and the measures taken up in the past by the researchers to overcome them. Focusing on the computational Fluid Dynamics part this paper discusses the pre- analysis methods, describing behind the scene mathematical approaches. Along with that the wall modelling strategies, which are of utmost importance in understanding the near wall behaviour of the fluid flow have been discussed. Various geometries with their uniqueness have been mentioned as a careful and accurate modelling of the missiles resulting in better aerodynamic calculations and for comparison and validation purpose. The next part discusses the handling of domain and the mesh for the WAFs. The physical setup and the boundary conditions are by and large the same, the computational step is briefly defined covering all the used turbulent models, their boundary conditions and the methods used for computing these models. In the end the validation and verification of the CFD process has been discussed in which the convergence parameters along with the range of the previously performed CFD analysis have been discussed. This paper will guide systematically the researcher in each step of the CFD analysis on WAFs.

2. AERODYNAMIC CHARACTERISTICS OF THE WAF MODEL

The aerodynamics of the WAF configuration are basically the nonlinear functions of the Mach number, angle of attack and the aerodynamic roll angle. The static stability at zero-degree angle of attack of missiles having WAF shows equivalent characteristics of planar fins having same cross section. The drag in WAF is greater than the planar fins of same cross section. The WAF induces a roll moment at 0° angle of attack and experience a side force moment at angle of attacks. A roll reversal is seen in the transonic regime near Mach 1. The cross derivatives do not appear to be significant below Mach number 2.5 [9]. A trend towards change of rolling moment is seen at the supersonic Mach numbers as well [10]. The various experimental and the computational studies have not been able to properly explain the roll reversal, however they have hinted towards the vortex formation at the fin body juncture on the convex side of the fin to be the cause for this anomaly. In some cases, the fins have been slotted to prevent roll reversal and in some cases the fins are housed in a cavity to negate the effect of “Magnus” moment present in the missile. A reliable stability analysis requires consideration of side moments due to classical Magnus effect and WAF both at the same time [11]. The WAF have an unconventional aerodynamics due to asymmetry; their roll damping stability derivatives show dependency upon the direction of the roll. The rolling moments are created because of the radial flow generated at the base of the fin. Future studies should also consider the out-of-plane side moment which is dependent on the pitch angle. The Magnus force, Magnus moment, and the Magnus effects have been comprehensively explained in the spinning and non-

spinning missile tests [12]. The wing curvature is found out to influence the yawing moment whereas the pitching moment, normal force, side force and the axial force remain unaffected by it. In comparison to the planar fins, the curved fins have significant effect in the yawing moment, rolling moment but a negligible effect on the normal force, side force and the axial force [13]. The supersonic flow around a WAF has been characterized near a single fin mounted on a semi cylindrical model, both numerically and experimentally. These experiments pave a new method for characterisation of flow field near the wrap-around fin.

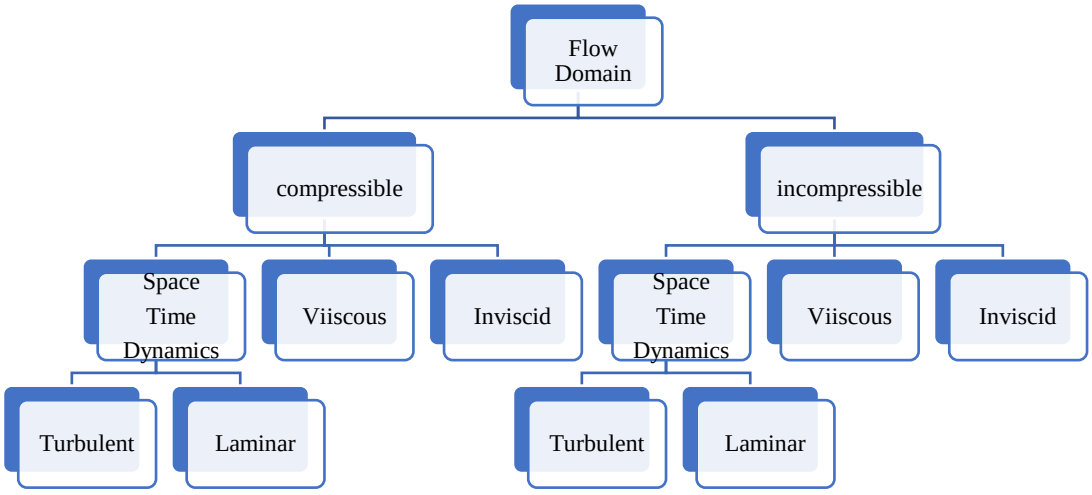

3. PRE-ANALYSIS/ MATHEMATICAL MODELS CFD APPROACH

The major classifications in the CFD models are compressible and incompressible flow domains, which are further illustrated in the hierarchy below. The CFD governing equations assume the flow to be quasi-one dimensional. The fundamental governing equations remain the continuity equation, the momentum equation and the energy equation.

Continuity equation:

$$\frac{\partial \rho}{\partial t} + \nabla.(\rho V) = 0 \tag{1}$$

Momentum equation:

$$\rho \frac{DV}{Dt} = \nabla.\boldsymbol{\tau_{ij}} - \nabla p + \rho \boldsymbol{F} \tag{2}$$

Energy equation:

$$\rho \frac{De}{Dt} + \rho(\nabla.\boldsymbol{V}) = \frac{\partial Q}{\partial t} - \nabla.\boldsymbol{q} + \boldsymbol{\Phi} \tag{3}$$

The general transport equations for mass, momentum, energy etc. which are solved on set of control volumes are:

$$\frac{\partial}{\partial t}\int_V \rho\phi dV + \oint_A \rho\phi \boldsymbol{V}.d\boldsymbol{A} = \oint_A \Gamma_\phi \nabla\phi.d\boldsymbol{A} + \int_V S_\phi d\boldsymbol{V} \tag{4}$$

where $\boldsymbol{\rho}$ is the fluid density, $\boldsymbol{V}$ is the fluid velocity vector, $\boldsymbol{\tau_{ij}}$ is the viscous stress tensor, $\boldsymbol{p}$ is pressure, $\boldsymbol{F}$ is the body forces, $\boldsymbol{e}$ is the internal energy, $\boldsymbol{Q}$ is the heat source term, $\boldsymbol{t}$ is time, $\boldsymbol{\Phi}$ is the dissipation term, and $\boldsymbol{\nabla . q}$ is the heat loss by conduction. Fourier's law for heat transfer by conduction can be used to describe $\boldsymbol{q}$ as:

$$\boldsymbol{q} = -k\nabla T \tag{5}$$

where $\boldsymbol{k}$ is the coefficient of thermal conductivity, and $\boldsymbol{T}$ is the temperature.

The energy equation (Equation 3) is a requirement of the compressible high-speed flow as it captures the shock pattern effectively. The majority of the WAF missiles flow in the turbulent conditions. The turbulence modelling involves selecting the near wall modelling approach and intrinsically defining the inlet and outlet conditions. Reynold number is a determining factor which defines the flow of the modelling.

$$\boldsymbol{Re_L} = \frac{\rho . U . L}{\mu} \tag{6}$$

where $\boldsymbol{L}$ is the length scale and μ is the kinematic viscosity. The transition to turbulence varies depending upon the type of flow;

External flow

- Along the surface : $Re_{Surface} > 50000$
- Around on obstacle: $Re_{Obstacle} > 20000$

Internal flow

- Internal : $Re_{internal} > 2300$

The basic computational approaches for turbulent flows are Direct Numerical Simulation (DNS), Large Eddy Simulations (LES) and the Reynolds Averaged Navier-Stokes Equation (RANS). The RANS approach is the most widely used approach in the wraparound missile simulations, best suited for complex geometries. Some of the early researches have also used an inviscid code for their simulations; however due to the new advancements and increasing computational capabilities, finding better possibilities using viscous and turbulent codes are in trend. The RANS based models are: the Spalart-Allmaras model, the $\mathrm{K}-\varepsilon$ family and the $\kappa-\omega$ family models, the Reynolds Stress Models and the Transition Models (i.e. the $\kappa-\kappa l-\omega$, transition shear stress transport (SST) models). These models are placed in order of cost increase calculated on iteration. The SST $\kappa-\omega$ and the Realizable $\mathrm{K}-\varepsilon$ are the recommended choices for the standard wraparound simulations. The shear stress transport (SST) is preferred where the boundary layers are critical and fine distinct resolved heat profiles are required. The near-wall treatment for the boundary layer profile prediction is done by making the velocity and the wall distance dimensionless. The velocity is made dimensionless, by dividing the velocity with shear velocity near the wall of the turbulent flow $\boldsymbol{U/U_\tau}$ where $\boldsymbol{U_\tau} = \sqrt{\frac{T_{wall}}{\rho}}$. The wall distance is made dimensionless $\boldsymbol{y^+} = \frac{\boldsymbol{yU_\tau}}{\boldsymbol{v}}$ where $\boldsymbol{y}$ is the distance from the wall and $\boldsymbol{v}$ is the dynamic viscosity of the fluid. A predictable boundary profile is obtained using these dimensionless quantities. The wall modelling strategies for the near wall treatment use the wall function approach in which a typical y^+ value is such that $30 < y^+ < 300$ and where resolving of viscous sub layer is required $y^+ \approx 1$ is set with the mesh growth rate not greater than ≈1.2, which is related directly to the inflation layers. In the wraparound fins the forces and the flow around the wall are important hence the recommended turbulence model in most of the cases is the SST $\kappa-\omega$. In various modified methods, SST $\kappa-\omega$ is used near the wall region and $\mathrm{K}-\varepsilon$ is used away from the walls. Assessment of various turbulent models

have been done in the past to improve the accuracy of the turbulent simulations. These models are Tam-Ganesan $K-\varepsilon$ model in which modification is done to accommodate heat effects in the turbulent jets, Tam-Thies $K-\varepsilon$, the standard Chien $K-\varepsilon$ and the Menter SST formulations; the modified RANS models represent the potential towards the accuracy of the turbulent methods and an approach towards experimentally observed data mean trends [14].

The basic two equation models fail to accurately predict the onset and amount of separation in adverse pressure gradient flows. Homogeneous turbulence, small Reynolds numbers, small pressure gradients etc. sometimes fail to correctly predict the aerodynamic flows. The $\kappa-\omega$ model in which the damping functions are not considered, allows simple Drichlet boundary conditions to be specified. It is unable to predict the asymptotic behaviour of the turbulence as it approaches the wall. In the $\kappa-\omega$ model the K and ε model-based distribution is inconsistent with the DNS data. The $\kappa-\omega$ model in the logarithmic region is superior to the $K-\varepsilon$ model. The logarithmic regions are important in the flows where we have moderate pressure gradients. The SST model accounts for the transport of the principal turbulent shear stress which clearly helps in accurately predicting the adverse pressure gradient conditions [15].

4. GEOMETRY

The Technical Cooperation Program (TTCP) model (Figure 1) has been widely used and accepted geometrical model for the WAF missile CFD analysis. All the dimensions are in respect of the radius or the diameters and in uniform calibres. A salient feature of this model which is adapted in most of the geometries is that the fins are pinched at 45°, both at the leading and trailing edges. The sharp edges provide a stark advantage over the blunt fins in terms of aerodynamics and the post processing visualisations. The edge shape has a significant effect on the roll moment of the wraparound fins. All dimensions are expressed in terms of calibres (1 calibre = 0.01524m) where as in scaled down models used in Jet Propulsion laboratory, California Institute of Technology, (JPL) dimensions were again expressed in terms of calibres (1 calibre = 0.1016m). The Aerial Delivery Research and Development Establishment [1] took (1 calibre = 0.2m) fins with symmetric pinched leading and trailing edges at 45˚. In the free flight tests [16] the scaled down TTCP model was adopted (1 calibre = 0.0191m). In the wind tunnel, water table and free flight tests [17] a rocket with the cavity housing was studied (1caliber = 0.122m). The symmetry of the body helps in testing only one fourth of the body with fin inclined at 45° from both the planes [18]. The thickness of the fin and the fin curvature are important parameters and should be considered in geometry modelling. The dimensions of the various previously used geometries with their unique features has been summarised in Table I. Based on 1 calibre = 0.01524m a missile model is shown in Figure 1, with the fin alone schematic of same calibre dimensions; however, the dimensions have been stated in mms so that accurate geometries can be designed in future.

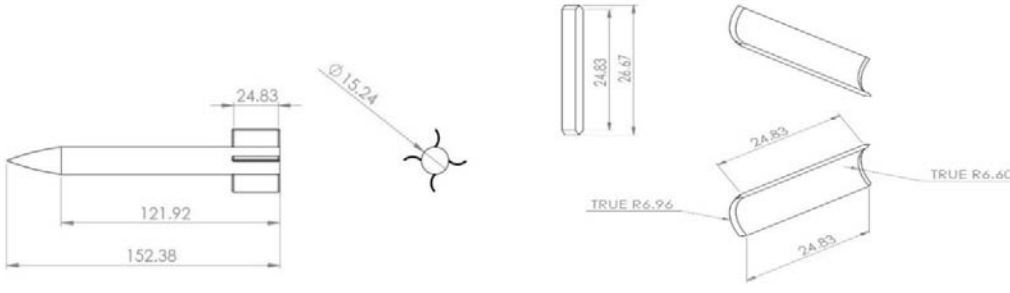

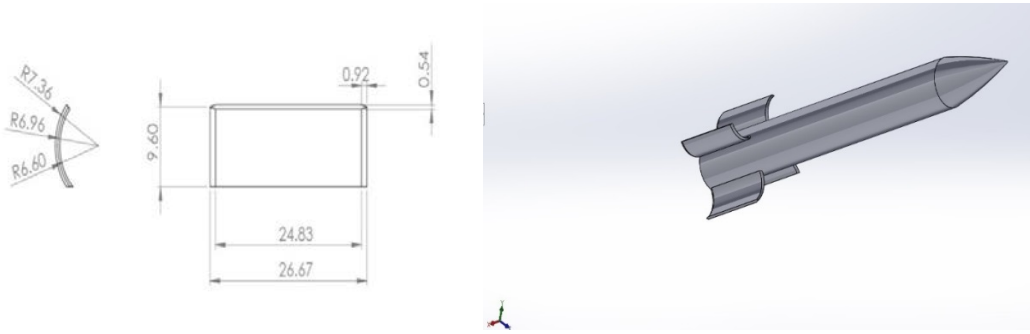

Figure 1: A standard model geometry with 1 caliber = 0.01524m, and detailed wraparound fin schematic, the dimensions are however shown in mm

Table I: Summarised geometry details

Reference	Geometry Type	Analysis type	Calibers	features
[1]	TTCP	CFD	1 Caliber = 0.2m	Both leading and trailing edges pinched at 45°
[4]	l/d of 20 & l/d of 17, cylindrical bodies with Von karman ogive noses	Both Experimental-Free flight tests and CFD	1 Caliber = 0.0143m	Short brass nose & long brass nose to simulate center of gravity in burnout condition
[5-9]	Single Fin test model	Both Experimental—Wind tunnel and CFD	1 Caliber = 0.0159m	Single fin, second-order continuity in the longitudinal direction ensured
[11]	US, Airforce institute, Ohio	Experimental/ Wind Tunnel	1 Caliber = 0.0191m	slotted
[17]	Airforce Armament laboratory	Experimental/ free flight tests	1 Caliber = 0.0191m	Slotted
[18]	Half scale of 122mm field rocket	Experimental/ Wind Tunnel, Water Table, Free Flight data	1 Caliber = 0.122m	Slender missile body with cavity housing
[19]	TTCP	CFD	1 Caliber = 0.1016m	Root & the Tip chord are parallel
[20]	TTCP	CFD	1 Caliber = 0.01524m	Symmetric leading and trailing edges at 45°
[20]	TTCP	CFD	1 Caliber = 0.01524m	Both leading and trailing edges pinched at 45°
[21]	Ogival nose	Experimental/ Wind Tunnel	-	Canted fins, in non zero roll orientation
[22]	ARF	Experimental/ free flight tests	1 Caliber = 0.01905m	Beveled Fins, with swept fins
[23]	Airforce Research Model	Experimental/ free flight tests	1 Caliber = 0.01905m	Missile body with base cavity
[24]	2.1 caliber Von Karman nose	Wind Tunnel	-	Body with High wing (concave side windward) and Low wing (convex side windward)
[25]	Infinitely long body	CFD	-	A 10% bi-convex airfoil shape, pinched at the end Fin aspect ratio of 2

In an interesting case a test model (Figure 2) was designed to represent a single fin of a typical WAF configuration. The model fin has the same proportions as free-flight models. It has a total length of 10.92r, where r = 0.0159m is the radius of curvature of the missile fin. Within this 5r length, a flat sur face is blended to a 1/3-cylinder section in such a way as to ensure second-order continuity in the longitudinal direction. This semi-cylindrical body has a length of 5.12r and a maximum height of 0.5r from the tunnel ceiling. The fin has a span of $\sqrt{2}$r, a chord length of 1.28r, a thickness of 0.2r. The fin is attached at the aft-most part of the cylinder

section, having the same radius of curvature as cylindrical body. Fin dimensions, as well as a bevelled leading edge, were chosen to match the free-flight models [5-9]. A schematic which can be used for future simulations is shown in Figure 3.

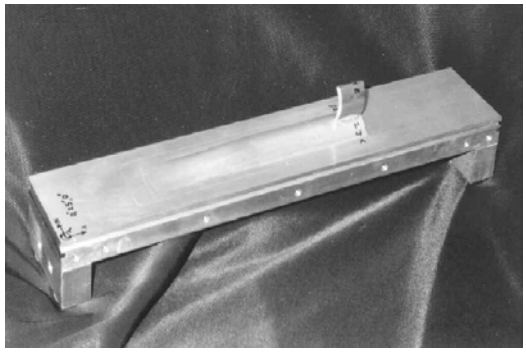

Figure 2: Single fin test model

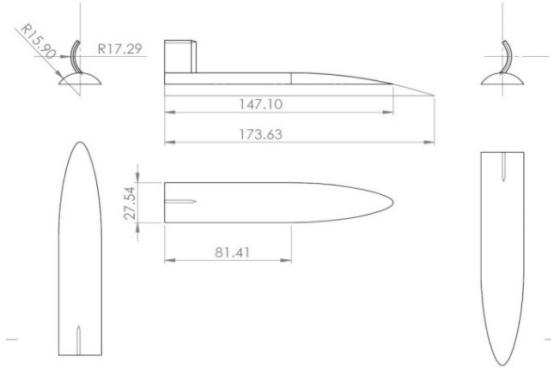

(a)

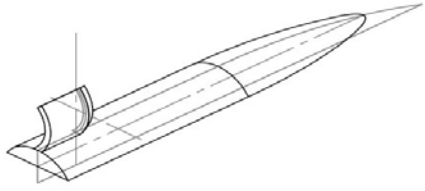

(b)

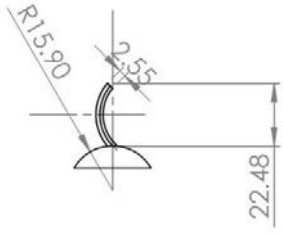

(c)

Figure 3: Single fin WAF test model (r = 0.0159m) dimensions shown are in mm

5. COMPUTATIONAL DOMAIN & MESH

The grid modelling is an essential as well as one of the most time-consuming step in CFD. For the accuracy of the computations, the boundary layer, the Y^+ and the mesh must be refined to the appropriate values, so that there are better flow field visualisations. The meshes used in the previous investigations are either structured, unstructured or a combination of both. The standard size of the computational field is kept ten times the size of the geometry, horizontally and 6 times the size of the geometry, vertically. This leads to enormous number of cells which may consume lot of time and resources while running the simulations. To solve this use of symmetry planes and non-reflecting boundary layers have been suggested, which decrease the number of cells significantly without compromising with the results. The mesh density needs to be focussed towards the nose and the fin region of the missile. The fin body juncture and the fin tips also need to be appropriately meshed. To solve this difficult meshing of fin juncture. A multi zone mapping method for mesh is described to capture the shocks accurately.[26] A tangent flow boundary condition is also applied in which the axial mapping is used. This method has given better results which have shown better agreement with the experimental results.

As the body is symmetric, one fourth missile body can be modelled (Figure 4) and the number of grids can be decreased. On using a non-reflecting boundary condition to the outermost grid plane from the boundary surface, very close outermost grid can be placed i.e. the computational domain can be reduced significantly thus helping in decreasing the computational times.

It should be noted that this is done only in case of analysing moment coefficients. In inviscid studies, a general trend has been seen of keeping the domain five times radially and ten times for upstream and downstream for accurate results. Due to the asymmetry of the WAF geometry a complete 4-Fin model is suggested in some works to study all the aerodynamic coefficients. Various computational domains have been applied, these include a single fin analysis (quarter of geometry), two adjacent fins model which emphasises on the “fin passage” area of the missile & a complete four fins model, having each their own set of pros and cons. A two fin, “fin passage” computational domain model is shown in Figure 5. For a single fin test model [5-9], a structured meshing was attempted as shown in Figure 6.

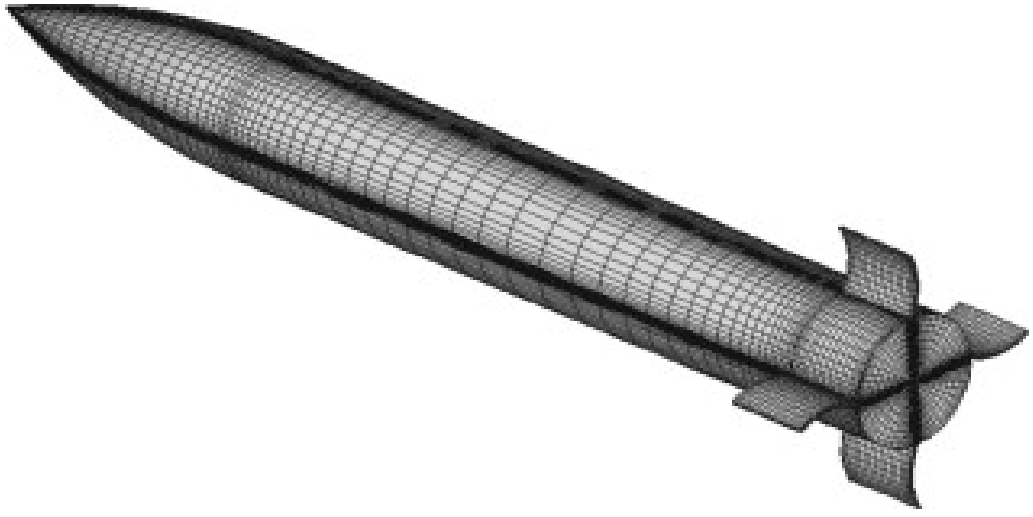

Figure 4: Using of symmetric one fourth body and non-reflecting boundary condition can help in reducing the grid points significantly

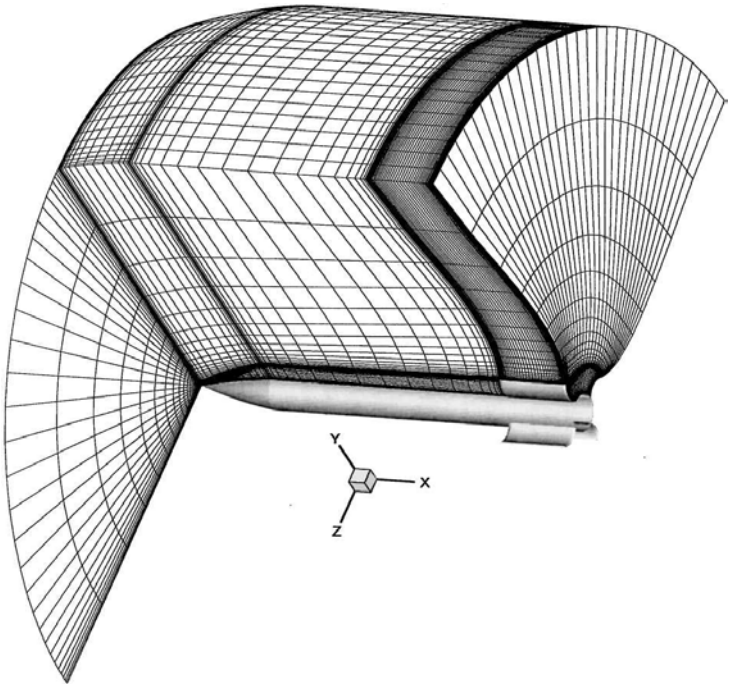

Figure 5: Two fin, Fin passage computational Domain model [20]

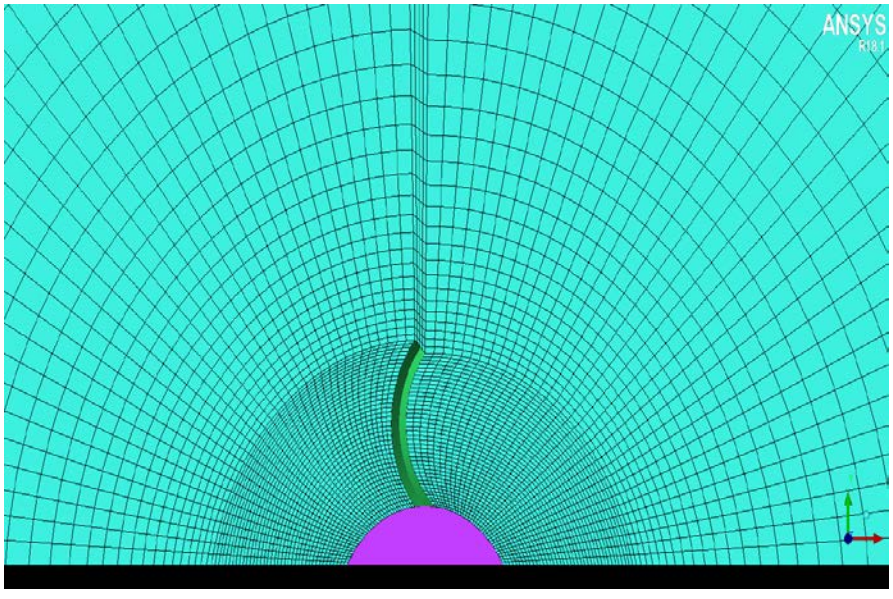

Figure 6: Grid boundaries and zonal Structures for single WAF configuration for a single fin based on references [5-9]

6. VERIFICATION OF THE GRID INDEPENDENCE

In most of investigations, utilization of three mesh systems for grid independence have been a standard protocol. The Drag coefficients were usually calculated against the Mach numbers. In certain cases, inviscid calculations have been performed estimating the surface pressure.

Table II: The Grid domain specification summary

Reference	**The Grid Domain/ Cell Numbers**			**The boundary Layer Y^+ value and the Growth Factor**	**Reference Area/ Body**	**Other mesh checking parameters**
[21]	Mesh 1	Mesh 2	Mesh 3	Height of the first Layer 1mm Growth factor height <1.15	$A_{ref} = \pi R^2$ and $L_{ref} = R$ where R is the rocket's radius.	Drag coefficient is compared at various Mach numbers.
	200Million	130Million	340Million			
	With variation in the results less than 2%, Mesh 2 with 130Million cells adopted.					
[1]	Optimum number of 0.3 Million was chosen. Grid independence done at 2.5M considering flow to be inviscid			-	-	Cylindrical computational domain of size 5 times Structured meshing employing Hexahedral map and Hexahedral cooper.
[4]	Multi Block ~ 1.5 million cells			0.0045 calibres	-	Grids orthogonally imposed and multi blocking Negligible Fin thickness
[19]	~ 1 million cells			-	One fourth body simulated	Highly clustered near the missile body
[26]	~0.4 million cells			-	Fin Aspect ratio kept 2	Focus on the fins only
[5]	~ 2.6 million cells			0.15	-	11 computational zones with 19 zonal boundaries connecting them Grids orthogonally imposed

7. INITIAL BOUNDARY & PHYSICAL CONDITIONS

The boundary conditions are used to solve the Euler and Navier-Stokes (N-S) equations numerically. These conditions are essential for the convergence of the solutions and the flow field accuracy. The boundary conditions involve: the inlet boundary condition, the outlet boundary condition and the wall boundary condition. The roll moment coefficients show dependency on the Reynold number hence should be taken care of.

Table III: The Initial Boundary & the Physical Conditions summary

Reference	**Inlet Boundary Condition**	**Outlet Boundary condition**	**Wall Boundary Condition**	**Control Volume conditions**			**Solver conditions**	**Other conditions**
[21]	Free Stream with far field boundary based on Riemann invariants reflecting boundary condition	Pressure outlet	No Slip, condition Sutherland Three coefficient formula for viscosity variation with the temperature	Free Stream Condition, Air: considered as an ideal gas	**Static Pressure** 101325 Pa	**Static Temperature** 288K	Density based couple solver	Advection Upstream Splitting Method (AUSM) based on Finite Volume Method (FVM), Second

								Order Upwind Scheme
[1]	Pressure inlet Absolute Velocity used	Pressure outlet	Model Surface as walls	Air as Ideal gas	1bar for M > 0.2	-	Steady state solution Coupled implicit formulation involving energy equation.	First order up winding scheme $K-\varepsilon$ model Green-Gauss cell gradient method varying Reynolds number from 27Million to 57Million at Mach 1.2 to 2.5
[4]	Velocity inlet	Velocity outlet		Inviscid flow conditions	-	-	Implicit, steady state Euler flow solver	Inviscid flow conditions
[19]	-	-	No Slip, condition	Freestream condition Density: 1.198 kg/m^3 Reynolds Number: 30-69 million for sea level & 17-69 million for wind-tunnel	101.3 kPa	294.75K	Explicit time marching method	Viscous flow Non-reflecting boundary conditions
[26]	-	-	Wall surface condition	Inviscid flow conditions	-	-	Euler based flow solver	-
[5]	Velocity inlet		Wall surface condition	0.2039 kg/m^3	217kPa	294K at Mach 2.9	Explicit solver	Inviscid First order accuracy with a full flux method

8. PRESENTATION OF THE NUMERICAL RESULTS

The solutions consist of both static and dynamic aerodynamic characteristics, and the data calculated is for the drag, lift, pitching moment, side moment and further their derivatives in terms of coefficients with respect to Mach number & angle of attack. The pressure contour plots at various Mach numbers have been dominantly used to analyse as well as predict the aerodynamic behaviour of WAF. Direct outputs have been used from the CFD to calculate the integrated forces and moments of the WAF missiles. Figure 7 is an example showing the difference in static pressure on concave and convex side of the fins which result in anomalies.

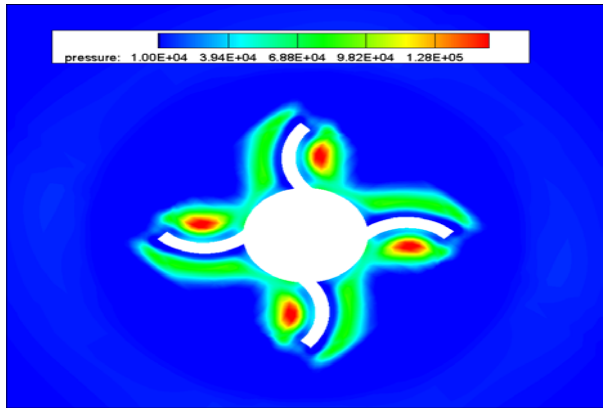

Figure 7: Pressure contours at Mach 5 [21]

The viscous and inviscid computations show different visualizations and different aerodynamics. Their roll- reversal Mach numbers also show variations. In case of a pinched fin missile, a conical shock at the projectile nose followed by an expansion wave and a relatively weaker shock is formed in front of the fins as compared to those having blunt fins. [1] To understand the flow between two fins (fins passage) Figure 8. Axial visualizations along the fins also portray the behaviour of the flow on the missile due to curved fins; this can be seen in Figure 9 at various fin lengths. Also, the CFD results of the single fin test model and their comparisons with the experimental results near single WAF at various Mach numbers are excellent visualizations for the understanding of flow on the curved fin surfaces. An attempt was made to analyse flow around a single fin both planar and curved, at Mach 2.5; the results of the pressure contours are shown in Figure 10.

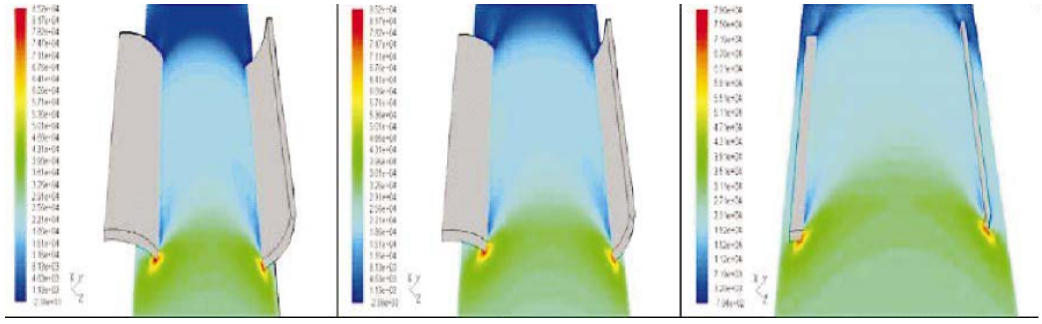

(a)

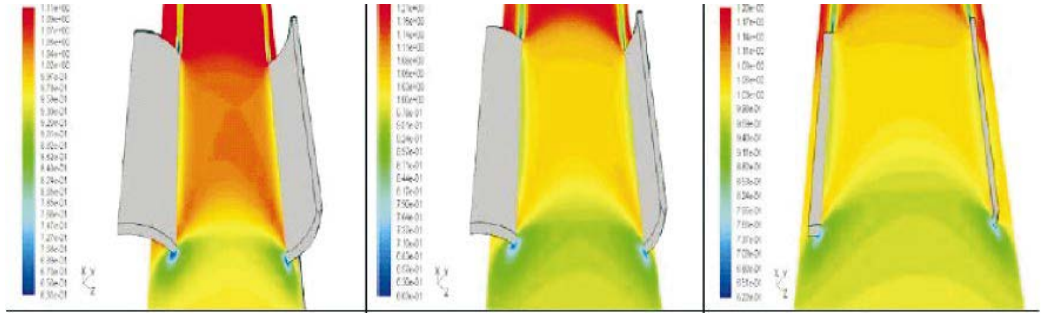

(b)

Figure 8: Mach number (a) and static pressure variations (b) in the fin passage at different span wise locations for free stream Mach number 1.4 [1]

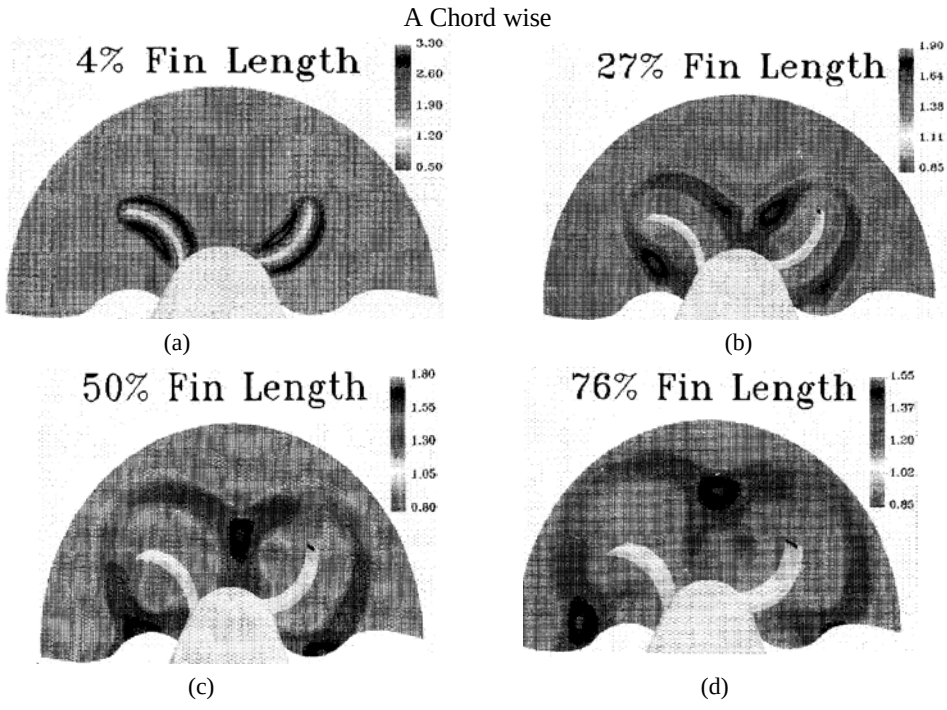

Figure 9: Normalised pressure contours at various axial positions on the fin lengths at 2.5 Mach [19]

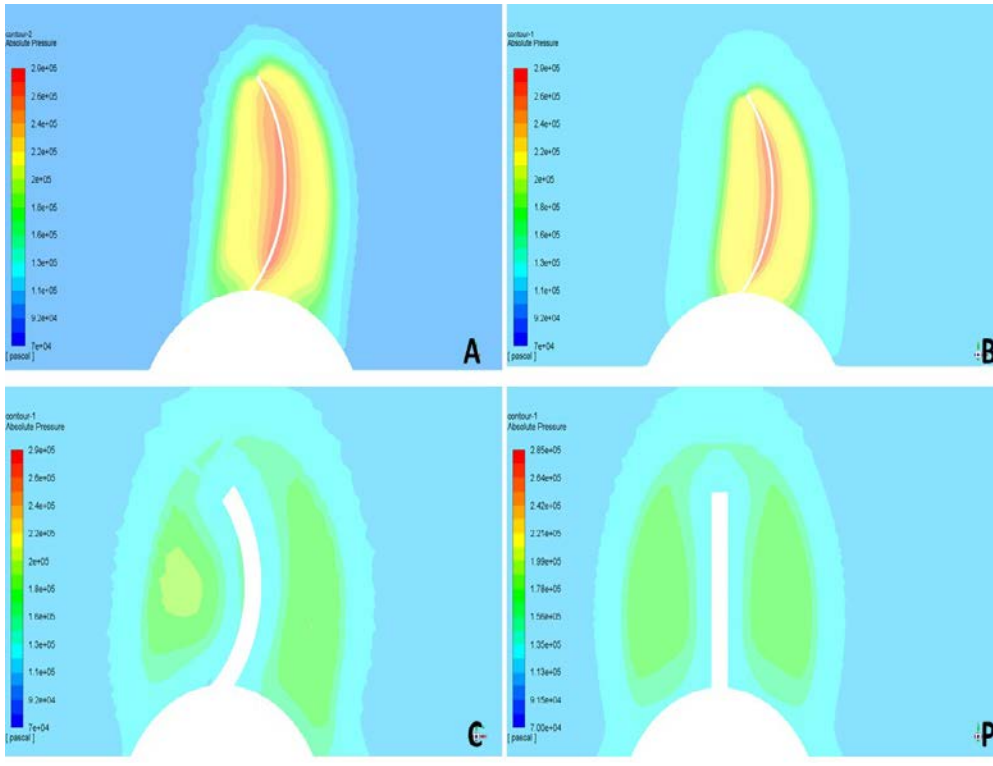

Figure 10: (A) & (B) Computed Pressure contours at the leading edge of single Wrap around Fin, (C) Computed Pressure Contours at the trailing edge of the curved Fin, (P) Computed pressure contours around a Single planar fin

9. VERIFICATION & VALIDATION OF THE CFD METHOD

For the verification of the CFD methods, the coefficients of Drag C_D, the coefficient of lift C_L, the rolling moment coefficients C_M are calculated against subsonic, transonic, & supersonic Mach number regimes. The models are investigated in various orientations i.e. fins being at 0° & 45° angle when viewed from the rear side. Though, most of the models are simulated at 0° calculations at various angle of attacks have also been performed. The CFD results have been validated with the experimental data, which mainly consist of results from the wind tunnel tests as well as the free flight tests. In the WAF system model having all the four fins should be solved however assuming it to be a case of an axisymmetric flow field only quarter of the geometry is considered as the domain and solved in some cases. Studies have also been performed on quarter of the missiles (referred as the fin passage) i.e. the region between the upper surface (concave side) of one fin and the lower surface (convex side) of the adjacent fin as the outer boundaries of the domain help in reducing not only the computational costs as well as insight of the WAF aerodynamics. The roll reversal of WAF configuration generally occurs around Mach 1, but in some simulations, it occurred at M= 1.8 [20].

Table IV: computational and experimental work summary for roll moments at Mach numbers

Data Source	Type of study	Range of Mach numbers	Roll reversal reported at Mach No.
[1]	CFD	1.2 – 2.5M	1.4M
[4]	Free flights & CFD	2-5.15M & 2-6M	4.5-4.7M
[5-9]	Experimental/Wind tunnel & CFD	3M & 5M	-
[11]	Experimental/ Wind Tunnel	2.15-3.83M	-
[14]	Experimental/ Wind Tunnel	1.7-4.0M	-
[17]	Experimental/ free flight tests	0.8-1.6M	-
[18]	Experimental/ Wind Tunnel, Water Table, Free Flight data	0.3-3.03M	-
[19]	CFD	1.3-3.0M	~1.7M
[20]	CFD	1.2-3.0M	1.8M
[21]	CFD	1.6-5M	1.9M
[22]	Experimental/ Wind Tunnel	0.5-2.0M	1.7M
[23]	Experimental/ free flight tests	1.5-3.0M	~1.0M (Stated)
[24]	Experimental/ free flight tests	0.6-1.8M	-
[26]	CFD	0.3-3.5M	~1M
[27]	Experimental/ free flight tests	0.6-1.35M	-

10. CONCLUSIONS

The WAF aerodynamics characterised in the previous studies has been reviewed in this paper with the focus on the CFD of WAF's. CFD is an effective tool in understanding the WAF aerodynamic anomalies. The new computational advancements allow us to use turbulent models economically. The modification of RANS turbulent methods leads to the corrections of the turbulent kinetic energy fields, the turbulent viscosity and thus should further be explored. In representation of the results the pressure contours help significantly in understanding the aerodynamic characteristics of the WAF model. The pressure on the concave surface is higher than the pressure on the convex surface which thereby produces the rolling moment, also termed as the induced rolling moment in some literature. The increasing

Mach number contours show that the shock waves at the nose become stronger and the shock wave angle becomes smaller gradually [21].

To understand the phenomenon behind this roll reversal, most of the CFD studies have correlated it with the pressure profiles, the shock structures, along with the increasing Mach numbers. Static pressure profiles against the Mach numbers have been studied both axially as well as parallel to the missile body at various chord lengths. The viscous flow over the curved fin surface opens a new set of flow dynamics which needs to be explored.

The SST based $K-\omega$ model should be a preferred turbulence model for the complex geometry simulations which shows superior results as compared to the other turbulent models. It is observed that at lower Mach numbers there is a negative value trend and at the higher Mach numbers there is a positive value trend for the roll moment coefficients. Many investigations have used inviscid flow solutions to save time in computations. These inviscid flow solutions may vary the aerodynamic results, therefore use of turbulent flow conditions is advised for accurate results. Even in the supersonic regime the aerodynamic characteristics such as the drag, roll show Mach number dependencies. Flights above Mach 3 show turbulent flow over the major parts of the missile body, imbedded in the laminar boundary flow; these hinder the accuracy of the Drag results in the CFD as compared to the flight tests. In this case choice of Reynolds number again plays an influential role [4], [19]. A multiple-zone strategy for meshing of WAF has shown results having better agreement with the experimental results. Applying of non-reflecting boundary layers and using one fourth domain help in reducing the grid elements and ultimately the computational time with no compromise in the accuracy of the results. A converging and diverging nozzle analogy after examining the chord-wise pressure have been suggested [25]. Rolling moment is a function of Mach number and the side force is linked with the roll angle of the missile. The Single fin semi-cylindrical model interprets the WAF aerodynamics excellently and show remarkable CFD as well as experimental results. The single fin semi cylindrical model can be utilized in both inviscid, viscous & turbulent CFD analysis. This paper can be used as a benchmark for future wraparound fin, CFD simulations which may help in better understanding of the wraparound fin aerodynamics.

REFERENCES

[1] A. Seginer, B. Bar-Haim, Aerodynamics of wraparound fins, *J. Spacecr. Rockets*, **20**, 339–345, doi:10.2514/3.25603, 1983.

[2] E. Air, F. Base, *Roll Motion of a Wraparound Fin Configuration at Subsonic and Transonic Mach Numbers*, 253–255, doi:doi:10.2514/6.1985-1777, 1986.

[3] G. L. Winchenbach, A. Branch, W. Riner, Aerodynamic test and analysis of a missile configuration with curved fins, *AIAA Paper 92-4495*, 1992.

[4] C. P. Tilmann, J. R. Huffman, T. A. Buter, R. D. W. Bowersox, *Characterization of the flow structure in the vicinity of a wrap-around fin at supersonic speeds*, 34th Aerospace Sciences Meeting and Exhibit, Reno, NV, U.S.A., 1996.

[5] J. R. Huffman, C. P. Tilmann, T. A. Buter, R. D. W. Bowersox, *Experimental Investigation of the Flow Structure in the Vicinity of a Single Wrap-Around Fin at Mach 2.9*, 1996.

[6] C. P. Tilmann, *Numerical and Experimental Investigation of the Flowfield Near a Wrap-Around Fin*, Dissertation, USAF/Wright Laboratory/Flight Dynamics Directorate, AFIT/DS/ENY/97-1.

[7] R. D. W. Tilmann, C. P., Huffman, Jr R. Buter, T. A. Bowersox, Experimental Investigation of the Flow Structure Near a Single Wraparound Fin, *Journal of Spacecraft and Rockets*, Vol. **34**, No. 6, pp. 729-736, https://doi.org/10.2514/2.3303, 1997.

[8] C. P. Tilmann, T. A. Buter, R. D. W. Bowersox, Characterization of the Flow field near a Wrap-Around Fin at Mach 2.8, *J. Aircr.* **35**, 868–875, doi:10.2514/2.2406, 1998.

[9] C. W. Dahike, *The Aerodynamic Characteristics of Wrap-Around Fins at Mach Numbers of 0.3 to 3.0*, Rep.

RD-77-4, U.S. Army Missile Command, Oct. 15, 1976.
[10] T. C. McIntyre, R. D. W. Bowersox, L. P. Goss, Effects of Mach number on supersonic wraparound fin aerodynamics, *J. Spacecr. Rockets*, **35**, 742–748, doi:10.2514/2.3410, 1998.
[11] O. Tannkulu, Wrap-Around Finned Missiles: Neat But Nasty, *AIAA-97-3493*, 108–126, doi:doi:10.2514/6.1997-3493, 1997.
[12] J. A. Struck, *Effects of Base Cavity Depth on a Free Spinning Wrap-Around Fin Missile Configuration*, (n.d.), doi:AHT/GAE/ENY/95D-22.
[13] W. Washington, *Experimental investigation of rolling moment for a body-wing-tail missile configuration with wrap around wings and straight tails at supersonic speeds*, 10th Atmos. Flight Mech. Conf., doi:doi:10.2514/6.1983-2081, 1983.
[14] N. Georgiadis, D. Yoder, W. Engblom, Evaluation of modified two-equation turbulence models for jet flow predictions, *AIAA J.*, 1–16, doi:10.2514/1.22650, 2006.
[15] F. R. Menter, Two-equation eddy-viscosity turbulence models for engineering applications, *AIAA J.* **32**, 1598–1605, doi:10.2514/3.12149, 1994.
[16] G. L. Abate and G. L. Winchenbach, *Aerodynamics of Missiles with Slotted Fin Configurations*, Aerodynamics Branch Aeromechanics Division Air Force Armament Laboratory Elgin AFB , Florida, 29th Aerospace Sciences Meeting, Aerospace, (n.d.).
[17] U. Catani, J. J. Bertint, S. A. Bouslog, Aerodynamic Characteristics for a Slender Missile with Wrap-Around Fins, *J. Spacecraft*, Vol. **20**, No. 2, 122–128, doi:doi:10.2514/6.1982-319.
[18] W. Fins, Computation of the Roll Moment for a Projectile With Wrap-Around Fins, *J. Spacecr. Rockets.* **31**, 615–620, doi:10.2514/3.26486, 1994.
[19] S.-K. Paek, T.-S. Park, J.-S. Bae, I. Lee, J. H. Kwon, Computation of Roll Moment for Projectile with Wraparound Fins Using Euler Equation, *J. Spacecr. Rockets.* **36**, 53–58, doi:10.2514/2.3432, 1999.
[20] M. Li, L. K. Abbas, X. Rui, The Simulation of Wraparound Fins' Aerodynamic Characteristics, *Wseas Transactions on Applied and Theoretical Mechanics*, **10**, 247–252, 2015.
[21] S. Mandic, Analysis of the Rolling Moment Coefficients of a Rockets with Wraparound Fins, *Sci. Rev. LVI*, 30–37, 2006.
[22] M. W. Swenson, G. L. Abate, E. Air, F. Base, R. H. Whyte, M. W. Swenson, R. H. Whytc, *AIAA-94-0200*, Aerodynamic Test and Analysis of Wrap-Around Fins at Supersonic Mach Numbers Utilizing Design of Experiments, 28th Aerospace Sciences Meeting & Exhibit, 1994.
[23] G. Abate, W. Hathaway, S. Burlington, A. T. Assoc, *AIAA 94-0051*, Aerodynamic Test and Analysis of Wrap Around Fins with Base Cavities, 32nd Aerospace Sciences Meeting 8th Exhibit, Test., doi:doi:10.2514/6.1994-51, 1994.
[24] E. F. Lucero, Subsonic Stability and Control Characteristics of Configurations Incorporating Wrap-Around Surfaces, *Journal of Spacecraft and Rockets*, **13**, 740–745. doi:10.2514/3.57135, 1976.
[25] G. Abate, T. Cook, Analysis of missile configurations with wrap-around fins using computational fluid dynamics, *Flight Simul. Technol.*, doi:doi:10.2514/6.1993-3631, 1993.
[26] A. B. Wardlaw, F. J. Priolo, J. M. Solomon, Multiple-zone strategy for supersonic missiles, *J. Spacecr. Rockets*, **24**, 377–384. doi:10.2514/3.25928, 1987.
[27] R. H. Whyte, W. H. Hathaway, G. E. Co, R. S. Buff, G. L. Winchenbach, R. H. Whyte, E. Air, F. Base, S*ubsonic and Transonic Aerodynamics of Wraparound Fin Configuration*, AIAA 23rd Aerospace Sciences Meeting, 1985.